Catalysis Letters 44 (1997) 247–253

Oxidation of propane to acetone and of ethane to acetaldehyde by O_2 in zeolites with complete selectivity

Hai Sun [*], Fritz Blatter [‡] and Heinz Frei [§]

Laboratory of Chemical Biodynamics, MS Calvin Laboratory, Lawrence Berkeley National Laboratory,
University of California, Berkeley, CA 94720, USA

Received 14 December 1996; accepted 29 January 1997

Oxidation of propane by O_2 to acetone was observed in solvent-free BaY and CaY under irradiation with visible light as well as under dark thermal conditions. The reaction was monitored in situ by FT-infrared spectroscopy. In the case of the photochemical oxidation, isopropyl hydroperoxide was detected as reaction intermediate. No byproduct was observed even upon $> 50\%$ conversion of the alkane. Ethane was oxidized completely selectively to acetaldehyde in CaY under irradiation with blue light.

Keywords: selective oxidation of ethane, selective oxidation of propane, photooxidation, zeolite BaY and CaY, alkane–oxygen charge-transfer

1. Introduction

Partial oxidation of small saturated hydrocarbons such as ethane and propane is a key challenge of current catalysis research. The underlying motivation is tapping of natural gas and volatile petroleum fractions as new feedstocks for important industrial chemicals [1–5]. For most large-scale processes, molecular oxygen is the only economically viable oxidant. However, product selectivities of reactions of low alkanes with O_2 are poor. The main reasons are the free-radical nature of these processes, the high exothermicity, and the fact that oxygen attacks partially oxidized products more easily than the starting hydrocarbon, resulting in overoxidation. The lack of product control is especially severe if the conversion is pushed beyond a few percent and constitutes the main obstacle towards direct transformation of low alkanes to organic building blocks and industrial intermediates by oxygen [2,4].

Most previously proposed approaches for ethane and propane oxidation by O_2 are based on catalysis over mixed metal oxides [6–11]. However, these systems produce large amounts of carbon oxide byproducts, some even at low conversion. Others tend to act mostly as oxidative dehydrogenation catalysts [12–15]. Still other solid oxide catalysts require irradiation with UV light, which poses limitations in terms of selectivity because of photofragmentation of primary products by these high-energy photons [16–18]. The same holds for partial oxidation of ethane by UV laser photolysis of supercritical ethane–O_2 mixtures [19]. Recently demonstrated electrochemical [20], transition metal [21,22], and iron porphyrin-based methods [23] all afford ethane or propane oxidation by O_2 but are accompanied by substantial amounts of carbon oxides or other carbon fragmentation products.

We have recently found that higher alkanes like cyclohexane or isobutane can be oxidized selectively by O_2 to corresponding alkyl hydroperoxide or its dehydration product (ketone) in zeolite NaY or BaY under visible light without photosensitizer [24,25]. This work led to attempts to achieve direct partial oxidation of low alkanes. Here we report completely selective oxidation of propane to acetone, and of ethane to acetaldehyde by oxygen at high conversion of the alkane. Reactions were conducted in BaY or CaY at ambient temperature under blue or green light. Dark thermal oxidation of propane to acetone was also achieved.

2. Experimental

2.1. General procedures

Zeolite BaY and CaY were prepared by repeated ion exchange of NaY (LZ-Y52, Aldrich Lot. No. 04724PZ) at 90°C in a 0.5 M solution of $BaCl_2$ or $CaCl_2$ [24–26]. Ion exchange was 97% in the case of BaY and 98% for CaY as determined by ICP. Self-supporting wafers of 8 mg of these materials were mounted inside a miniature vacuum cell that allowed in situ infrared monitoring of the reaction (FT-infrared spectrometer IBM-Bruker model IR-44). The wafers were dehydrated at 200°C under vacuum (Varian model V-70 turbomolecular pump) for about 10 h before loading of alkane and O_2 from the gas phase. The miniature vacuum cell was

---

[*] Present address: Memc Corporation, St. Louis, MO, USA.
[‡] Present address: Ciba-Geigy, Basel, Switzerland.
[§] To whom correspondence should be addressed.

mounted inside a variable temperature vacuum system with a tuning range from 77 K to 200°C (Oxford model DN1714). The loading level of alkane and O_2 was controlled by gas pressure and zeolite temperature. For photolysis, a prism-tuned Ar-ion laser Coherent model Innova 90-5 or a conventional tungsten lamp as used. The emission of the lamp was limited to the visible by a UV cut-off filter.

For determination of the conversion of propane or ethane, known amounts of the alkane and the final products acetone or acetaldehyde were loaded into BaY or CaY in a series of separate experiments. Quantities adsorbed were measured manometrically. At room temperature and several hundred Torr of propane or ethane, the gas phase hydrocarbon in the miniature cell contributes significantly to the observed infrared spectrum. The gas phase bands were removed by spectral subtraction, and the infrared extinction coefficient of the alkanes were measured by lowering the pellet temperature to -100°C, thereby inducing quantitative adsorption into the zeolite pores. Extinction coefficients of infrared bands of the isopropyl hydroperoxide were determined from difference spectra recorded upon thermal interconversion of the hydroperoxide intermediate to acetone and H_2O.

Propane (Matheson, 99.7%) and ethane (Phillips Petroleum, 99.99%) were treated by trap-to-trap distillation on a vacuum line before use. Propane-d_8 (Cambridge Isotope Laboratories, 98%), ethane-d_6 (Cambridge Isotope Laboratories, 98%), ethane-$^{13}C_2$ (Isotech Inc., 99.1%), and oxygen gas (Air Products, 99.997%) were used as received.

2.2. Residual water in zeolite

We expected the photochemical and thermal reactivity of alkanes in alkaline-earth zeolite Y to be sensitive to the concentration of residual water. Therefore, a series of experiments was conducted to determine the concentration of remaining H_2O in our BaY and CaY pellets after a typical dehydration procedure. An ideal infrared absorption of water for these measurements is the relatively narrow and moderately intense bending mode at 1640 cm^{-1}. In order to determine the extinction coefficient of this band, small, known amounts of water vapor (measured by manometric techniques) were adsorbed into the dehydrated zeolite and infrared spectra recorded. The weight of the pellet was obtained by transferring it after the infrared measurement into a closed glass container of 100% humidity. Leaving the pellet for several days in this environment ensured complete hydration. The weight of the dry pellet was calculated from that of the hydrated zeolite by assuming 26% water content (by weight) [27]. From these data and the known density of supercages in zeolite Y (3.8×10^{20} g^{-1}) [27], the number of H_2O molecules per supercage was calculated. Results are close to those reported for the extinction coefficient of the H_2O infrared bending mode in zeolite NaY reported by Bertsch and Habgood [28]. We found a loading level of 0.3 H_2O molecules per supercage of BaY or CaY following our standard treatment of 10 h dehydration at 200°C under high vacuum. Figure 1 shows the H_2O bending absorption at 1640 cm^{-1} with the intensity of each spectrum normalized to one H_2O molecule per supercage. Note that the integrated intensities are about the same in all three zeolites, although the band is appreciably broader in CaY than in BaY or NaY. Using this infrared method, water levels could easily and accurately be varied.

3. Results and discussion

3.1. Visible light-induced oxidations

When loading a pressed pellet of dehydrated zeolite BaY with 150–300 Torr propane and 1 atm of O_2 gas, no reaction was noted in the dark at ambient temperature. By contrast, chemical reaction was observed when irradiating the zeolite pellet with blue or green light of the tungsten lamp or the continuous-wave Ar ion laser. An infrared difference spectrum showing reactant depletion and product growth following 150 min photolysis at 488 nm (500 mW cm^{-2}) is presented in figure 2. All product absorptions (positive bands) can be attributed to either acetone, water, or propyl hydroperoxide. Identification of acetone (1247, 1365 (shoulder), 1374, 1418, 1684, 1707 cm^{-1} (shoulder)) and H_2O (1650, 3470 cm^{-1} (broad)) is based on comparison with infrared spectra of authentic samples loaded into BaY. All other product bands (1270, 1318, 1348, 1374, 1391, 1456, 1472, 3170 cm^{-1} (broad)) decrease at ambient temperature in the dark under concurrent growth of $(CH_3)_2C{=}O$ and H_2O. Therefore, this thermally unstable intermedi-

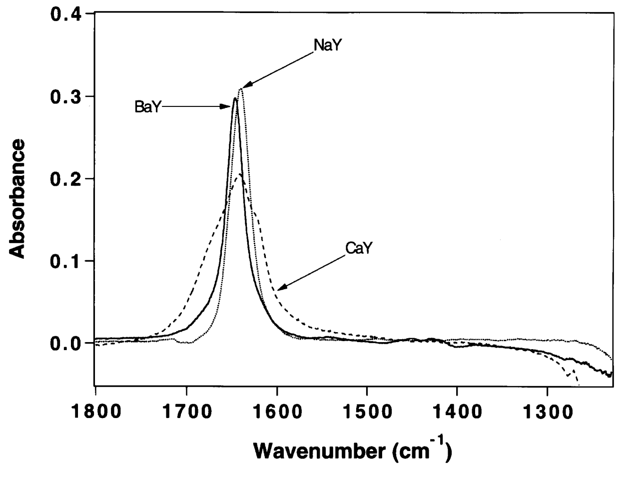

Figure 1. FT-infrared spectra of NaY, BaY, and CaY pellets in the H_2O bending region upon loading of water from the gas phase. Spectra are normalized to one water molecule per supercage.

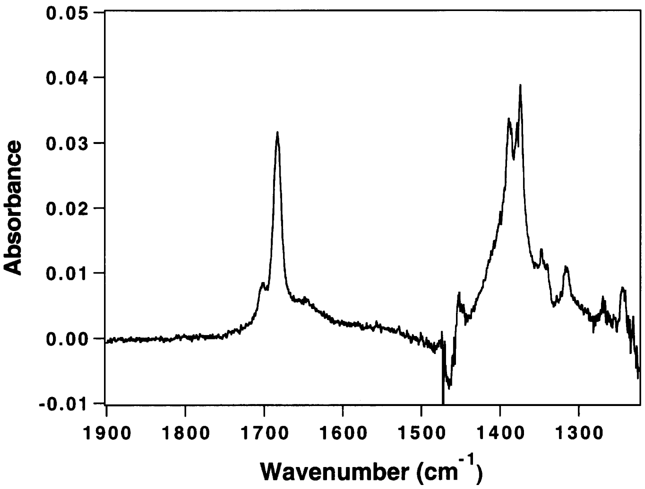

Figure 2. Photooxidation of propane. FT-infrared difference spectrum before and after irradiation at 488 nm (500 mW cm^{-2}) for 150 min at room temperature of a zeolite BaY pellet loaded with 300 Torr of propane and 650 Torr of O_2 gas.

ate has the composition $C_3H_8O_2$. The broad absorption at 3170 cm^{-1} is characteristic for alkyl hydroperoxides in zeolite BaY [24,25], and the bands in the fingerprint region agree well with alkyl hydroperoxide IR spectra reported in the literature [29]. Hydroperoxides with a H in a position have been shown to rearrange thermally to carbonyl compound and H_2O at ambient temperature [25]. We conclude that the thermally labile product is propyl hydroperoxide. While distinction between primary and secondary propyl hydroperoxide cannot be made on the basis of the infrared data alone, the observed elimination of H_2O to yield acetone allows us to identify unambiguously the intermediate as isopropyl hydroperoxide. No other product was observed even when monitoring the photochemistry up to 22% conversion of the propane and following the subsequent rearrangement of the isopropyl hydroperoxide intermediate to acetone. The conversion was calculated as the ratio of total product growth to amount of propane loaded into the zeolite matrix (see section 2.1). Analogous experiments with propane-d_8 confirmed acetone and water as the only final photolysis products.

Oxidation of ethane by O_2 was observed in Ba^{2+}- and Ca^{2+}-exchanged zeolite Y. No thermal reaction occurred when loading 250–500 Torr ethane and 1 atm of O_2 into the dehydrated zeolite pellet. Compared to propane oxidation, photochemical reaction of ethane under visible light from a tungsten lamp or blue light from an Ar ion laser (488 nm) was slow in BaY. The product yield increased four-fold when conducting the reaction in zeolite CaY instead. An infrared difference spectrum of blue light driven ethane oxidation in CaY is shown in figure 3. Readily observed product bands at 1357, 1419, 1707, and 1716 cm^{-1} (shoulder) originate from acetaldehyde, while the absorption at 1654 and 3400 cm^{-1} is due to H_2O. These assignments were confirmed by recording of ethane-d_6 photooxidation in CaY. Identification of acetaldehyde was based on comparison with infrared spectra of authentic $CH_3CH{=}O$ and $CD_3CD{=}O$ samples in CaY. No final product aside from acetaldehyde and H_2O was observed even at the highest recorded conversion (20%). Specifically, no CO_2 was produced, a major byproduct of any other method for ethane oxidation by O_2. This finding was confirmed by experiments using $^{13}C_2H_6$. $^{13}CO_2$ has an asymmetric stretch absorption that is removed by a red shift of 65 cm^{-1} from the absorption of atmospheric carbon dioxide traces in the spectrometer optical path.

Acetaldehyde growth upon photolysis exhibits an

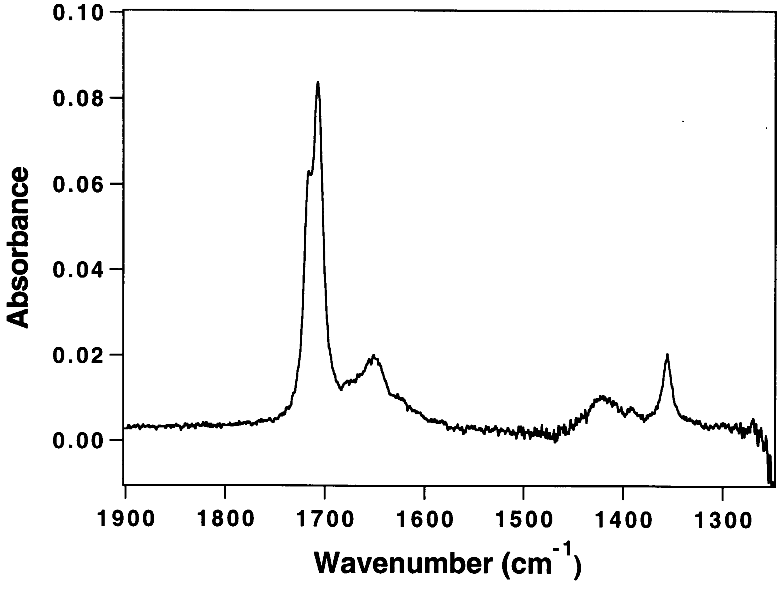

Figure 3. Photooxidation of ethane. FT-infrared difference spectrum before and after irradiation at room temperature of a zeolite CaY pellet loaded with 500 Torr ethane and 750 Torr O_2 gas at 488 nm (500 mW cm^{-2}) for 180 min.

induction period as shown in figure 4. This suggests that the aldehyde is formed via an intermediate. Indeed, when removing excess ethane and O_2 from the zeolite after photolysis and monitoring the matrix for several hours in the dark at room temperature, a slow growth of acetaldehyde and H_2O was observed under concurrent decrease of very small bands at 1282, 1391, 1488, and 3200 cm^{-1} (shoulder). The final products acetaldehyde and H_2O strongly suggest that the observed intermediate is ethyl hydroperoxide, and the infrared spectrum is consistent with this assignment [29]. We conclude that ethyl hydroperoxide is most likely the primary photoproduct of blue light induced ethane oxidation by O_2 in CaY which thermally eliminates H_2O to yield acetaldehyde as sole final oxidation product.

The most probable origin of the visible light-induced reaction of propane and ethane with oxygen is excitation of the alkane·O_2 charge-transfer state. We found recently that when loading higher alkanes such as cyclohexane or isobutane together with O_2 gas into zeolite BaY or NaY, reflectance measurements give an optical absorption tail extending into the green spectral range (500 nm). This tail is attributed to the hydrocarbon·O_2 contact charge-transfer transition [24,25]. The onset of the corresponding absorption in high-pressure O_2 gas phase or O_2-saturated liquid alkane lies in the UV region below 300 nm [30]. This implies a 2–3 eV red shift of the absorption onset in the zeolite. The large shift is caused by a strong stabilization of the polar charge-transfer state (alkane radical cation–O_2^- pair, dipole approximately 15 D) by the high electrostatic field inside the zeolite cage. Zeolite Y has a three-dimensional network of 13 Å diameter cages which are connected by 8 Å windows. The wall of each cage carries a formal negative charge of 7, which is counterbalanced by 3–4 Ba^{2+} ions located inside the cage. These cations are poorly shielded and hence give rise to very high fields inside the cage [25,31–33]. We have determined the electrostatic field in BaY experimentally by measuring the induced infrared fundamental absorption of N_2 and O_2 gas loaded into the zeolite [34]. These infrared forbidden modes become active in the presence of the cage electrostatic field, and the magnitude of the field can be determined form the band intensity [35]. The average field experienced by these molecules inside the cages of BaY is 0.8 V $Å^{-1}$. The stabilization of a 15 D dipole aligned parallel to this field would be 3 eV ($-\mu \cdot \boldsymbol{E}$). This rough estimate of the stabilization of the charge-transfer state by the cage electrostatic field is in good agreement with the observed red shift of the cyclohexane·O_2 and isobutane·O_2 absorption tail in zeolite Y. Although the higher ionization potentials of propane and ethane prevent us from direct detection of the alkane·O_2 charge-transfer absorption tail by reflectance spectroscopy in these cases, the observed trend of the reaction yields is consistent with the charge-transfer interpretation. Specifically, we found that the product yield per photon at fixed photolysis wavelength (488 nm) scales inversely with the ionization potential of the alkane (isobutane, 10.6 eV; propane, 11.1 eV; ethane, 11.5 eV). We conclude that the trend of the product yields among the alkanes in BaY suggests a common mechanistic origin, namely, excitation of the hydrocarbon·O_2 charge-transfer state which is strongly stabilized by the electrostatic field of the zeolite cage.

The initial step following excitation of the charge-transfer state is most likely fast proton transfer from the propane (ethane) radical cation to O_2^- to yield an alkyl radical and HO_2 radical (scheme 1). Propane and ethane radical cations are spectroscopically established species [36]. Alkane radical cations in general are known to be

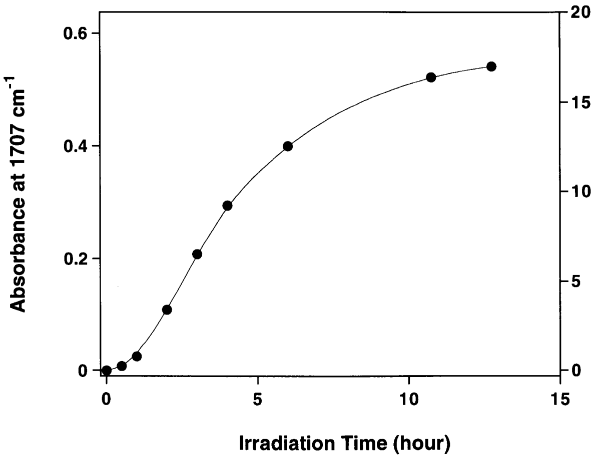

Figure 4. Acetaldehyde growth kinetics at 1707 cm^{-1} (C=O stretch) upon irradiation at 488 nm (800 mW cm^{-2}) of a CaY pellet loaded with 250 Torr of ethane and 750 Torr of O_2.

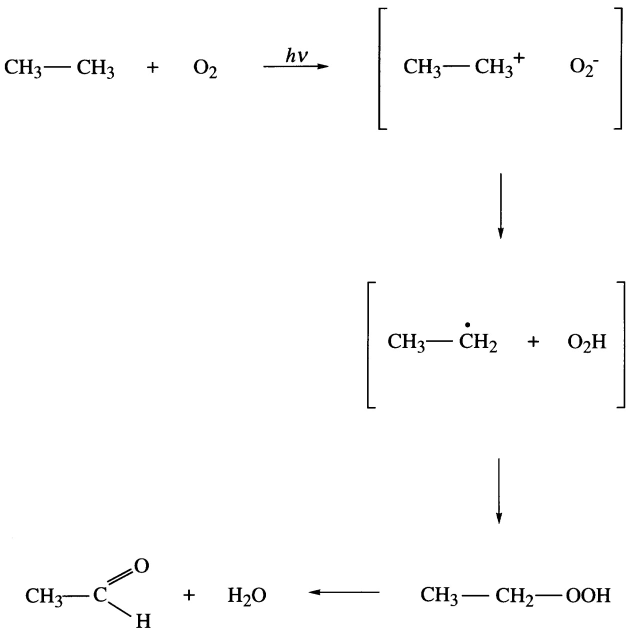

Scheme 1. Proposed mechanism for alkane photooxidation.

highly acidic and therefore have a very strong tendency for proton transfer to a base like O_2^- [37]. Coupling of the cage radical pair so produced would yield isopropyl (ethyl) hydroperoxide. Heterolytic thermal rearrangement of the hydroperoxide to carbonyl product and H_2O is a process observed for all alkyl hydroperoxides with a H in α position [25].

The increase of the photochemical yield of ethane oxidation upon substitution of BaY by CaY is consistent with the higher electrostatic fields in the CaY cage [31,32] as this results in a stronger stabilization of the ethane·O_2 charge-transfer state. However, while zeolite BaY can be prepared free of acid sites, this is not possible for CaY; the latter inevitably contains Brønsted acid sites [38,39]. We cannot rule out that these sites play a role in the reaction mechanism, although we have no evidence for it. Whether the acid sites of CaY influence the reaction path or not, the product selectivity in the case of the ethane oxidation is not affected by them in any way.

3.2. Thermal oxidation of propane in CaY and BaY

Upon loading of propane and O_2 into zeolite CaY, thermal reaction was noted at room temperature just minutes after introducing the gases into the pellet. Figure 5 shows an infrared difference spectrum taken 5 h after loading of 150 Torr propane and 1 atm O_2 into CaY. Product bands at 1700, 1689, 1420, 1375, 1365, and 1246 cm^{-1} originate from acetone as confirmed by comparison with the infrared spectrum of an authentic sample of the ketone in CaY and by literature spectra [40,41]. The band at 1640 cm^{-1} and a very broad absorption centered around 3400 cm^{-1} are due to H_2O coproduct. No other product grew in. We conclude that propane is oxidized in the dark by O_2 to acetone with complete selectivity. It is important to note that propane was completely inert in CaY as long as no O_2 was added to the zeolite.

The 1700/1689 cm^{-1} doublet of the C=O stretching absorption of acetone is attributed to two different sites of the molecule in the zeolite cage. At the earliest stage of the reaction, only the 1689 cm^{-1} band grows in. The 1700 cm^{-1} peak appears upon continued accumulation of acetone. The same phenomenon is observed when loading an authentic sample of acetone from the gas phase, which confirms that the strong ν(C=O) product absorption originates exclusively from acetone.

Acetone absorbance growth at ambient temperature (figure 6) shows about 20% conversion of propane during the first 10 h after loading of propane into the zeolite. This was achieved in a CaY pellet with 0.3 H_2O molecules per supercage (curve 1). Dark growth levels off after that, but irradiation with blue light results in a new sharp increase of the yield, also shown in figure 6. We monitored the reaction up to 30% conversion of the alkane without noticing any degradation of the product selectivity. The residual water content strongly influences the thermal reaction as illustrated by curve 2 of figure 6; it shows the acetone product growth in a CaY pellet with 1.1 H_2O molecules per supercage under otherwise identical conditions as in trace 1.

No thermal oxidation of propane was observed in zeolite BaY at ambient temperature, even when exposing the pellet to 8 atm of O_2 for 10 h. However, very slow dark reaction was noticed at 55°C, and the rate increased sharply towards higher temperature. Acetone absorbance growth curves for 55, 90, and 150°C runs are displayed in figure 7. At 150°C, one third of the propane in the zeolite is converted in 9 h, with acetone as the exclusive product. No loss of selectivity was observed upon subsequent irradiation with blue light for another 2 h,

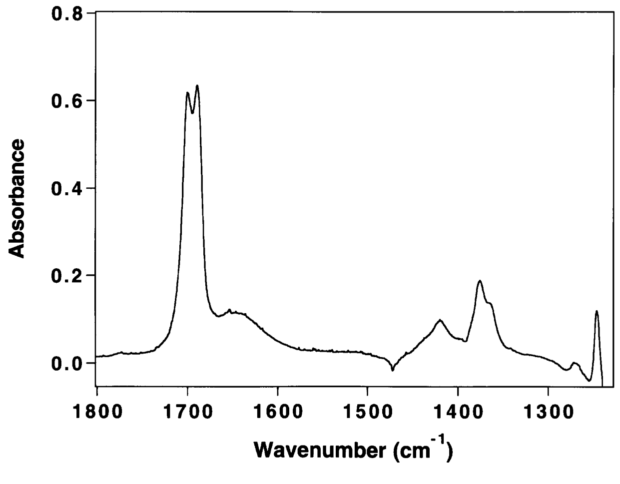

Figure 5. Thermal oxidation of propane. FT-infrared difference spectrum after 5 h reaction at 21°C in a CaY pellet loaded with 150 Torr propane and 1 atm O_2.

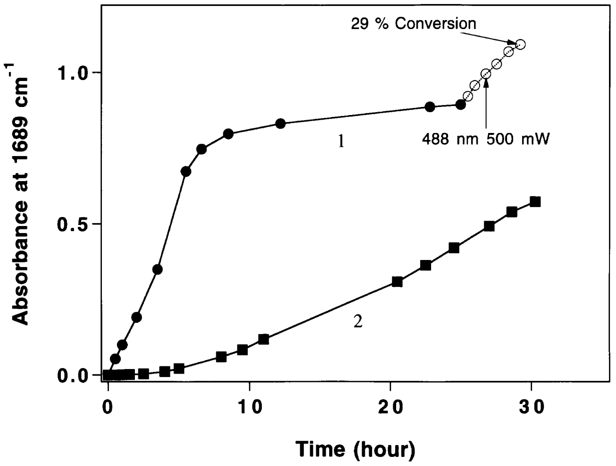

Figure 6. Kinetics of thermal propane oxidation in CaY at room temperature. Curve 1 shows acetone growth due to spontaneous oxidation in a pellet with 0.3 residual H_2O molecules per supercage (filled circles), followed by blue light-induced growth (open circles). Curve 2 gives the thermal product growth in a CaY pellet containing 1.1 H_2O molecule per supercage. Propane pressure, 150 Torr; oxygen, 750 Torr.

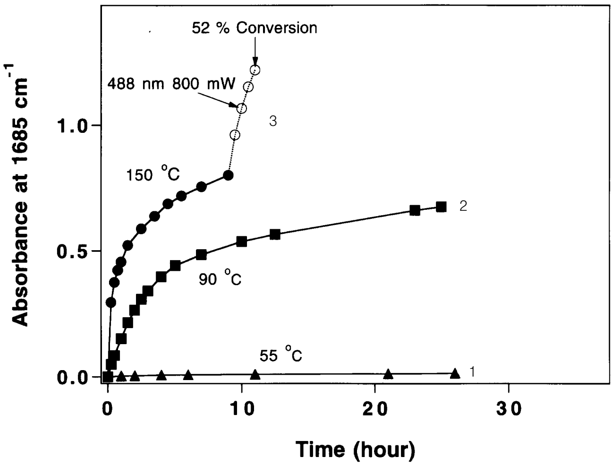

Figure 7. Kinetics of thermal propane oxidation in BaY at elevated temperatures. Curve 1 shows acetone growth at 55°C in a pellet with one residual H_2O molecules per supercage. Curve 2, at 90°C. Curve 3 represents thermal growth at 150°C (filled circles), followed by blue light-induced oxidation (open circles). Propane pressure, 150 Torr; oxygen, 750 Torr.

reaching 52% conversion of the alkane. It is clear from the steep slope of the top growth curve in figure 7 that there is no sign of leveling off even at that point. In the case of zeolite NaY, no thermal autoxidation of propane was observed at temperatures as high as 150°C.

There are a few reports on thermal oxidation of a larger alkane, namely cyclohexane, by oxygen gas in cation-exchanged zeolite Y. Ukharskii et al. noted infrared product absorptions at 1720, 1780, and 1820 cm^{-1} upon oxidation in NaY at temperatures as low as 60–80°C, indicating ketone and other products (possibly anhydride) [42]. Thermal cyclohexane oxidation in NaY producing exclusively cyclohexyl hydroperoxide and cyclohexanone (its dehydration product) was observed in the temperature range from 20–80°C in our laboratory [25]. Vanoppen et al. conducted a systematic study of cyclohexane autoxidation in alkali and alkaline-earth zeolite Y (NaY, BaY, SrY, CaY) at 80°C [43]. Increased reactivity was observed in this order, and in situ monitoring by diffuse reflectance FT-IR revealed cyclohexanone and H_2O as initial products. Continued reaction resulted in growth at 1580 cm^{-1}, assigned to a carboxylate product, but this secondary reaction was less pronounced for the more active, alkaline-earth zeolites [43].

While still speculative, our observations in the case of cyclohexane autoxidation in NaY nevertheless point to a charge-transfer mechanism involving cation sites with especially strong electrostatic fields (there is a heterogeneity in terms of cation shielding, as discussed in more detail in our previous paper) [25]. It is the high mobility of alkane and oxygen molecules in the zeolite that allows easy access to such minority sites. At these most poorly shielded cation sites, spontaneous charge-transfer could result in alkane radical cation and O_2^- formation. The fact that this process occurs in zeolite NaY with cyclohexane but not with propane is consistent with the considerably lower ionization potential of cyclohexane (9.8 eV) compared to propane (11.1 eV). Moreover, our observation that propane reacts faster in CaY than in BaY, and not at all in NaY is consistent with the increasing fields in NaY < BaY < CaY. The effect of the concentration of residual water in the zeolite reflects the shielding of coulombic interactions by H_2O. All these findings support charge-transfer from alkane to O_2 as the initial reaction step. However, as mentioned above, CaY invariably contains acid sites that may play a role in the mechanism in this zeolite. We envision the same mechanism for the subsequent reaction leading to alkyl hydroperoxide and ketone as proposed in the case of photochemical oxidation (analogous to scheme 1). At elevated temperatures, chain propagation may play a role (scheme 2) as sufficient energy is available to overcome the 18 kcal mol^{-1} activation energy for H abstraction from alkane [44].

Interesting is the finding that there is efficient photo-induced propane oxidation even after the thermal growth has leveled off (figures 6 and 7). We interpret this as evidence that photochemical reaction occurs in the majority of the supercages, while initiation of thermal reaction is restricted to a small number of cages with exceptionally large fields. The latter may become shielded as the polar products (acetone, H_2O) accumulate, thus preventing further reaction at these sites. Nevertheless, the conversion is high even for the thermal reaction (35% in BaY at 150°C (figure 7)).

4. Conclusions

This work demonstrates visible light driven oxidation of propane and ethane to the corresponding carbonyl product and its alkyl hydroperoxide precursor by oxygen in alkaline-earth zeolite Y. Propane oxidation was also accomplished thermally at mild temperatures, with acetone as the sole oxidation product even at high conversion of the alkane. This is the first time that low alkane oxidation by O_2 to carbonyl without byproduct has been achieved. It opens the possibility of using propane and ethane, both constituents of natural gas, as new feedstocks for acetone and acetaldehyde in place of

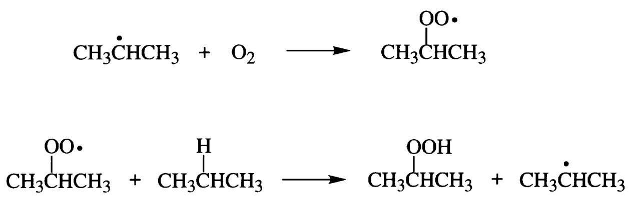

$$\mathrm{CH_3\dot{C}HCH_3 + O_2 \longrightarrow CH_3\overset{OO\bullet}{C}HCH_3}$$

$$\mathrm{CH_3\overset{OO\bullet}{C}HCH_3 + CH_3\overset{H}{C}HCH_3 \longrightarrow CH_3\overset{OOH}{C}HCH_3 + CH_3\dot{C}HCH_3}$$

Scheme 2. Proposed chain propagation upon thermal propane oxidation.

propene (ethene). More generally, the reactions furnish a method for highly selective C–H activation of low alkanes under very mild conditions.

Acknowledgement

This work was supported by the Director, Office of Energy Research, Office of Basic Energy Sciences, Chemical Sciences Division of the US Department of Energy, under Contract No. DE-AC03-76SF00098. The authors thank Dr. D.L. Vanoppen and Professor P.A. Jacobs for a preprint of ref. [43] and helpful comments regarding the mechanism of the thermal alkane oxidation.

Supplementary information

FT-infrared spectra supporting the product identification described in the manuscript are available from the authors upon request.

References

[1] R.A. Sheldon and J.K. Kochi, *Metal-Catalyzed Oxidation of Organic Compounds* (Academic Press, New York, 1981) ch. 11.
[2] C.B. Dartt and M.E. Davis, Ind. Eng. Chem. Res. 33 (1994) 2887.
[3] C.L. Hill, ed., *Activation and Functionalization of Alkanes* (Wiley, New York, 1989).
[4] J.E. Lyons and G.W. Parshall, Catal. Today 22 (1994) 313.
[5] G. Centi, Catal. Lett. 22 (1993) 53.
[6] Y.C. Kim, W. Ueda and Y. Moro-oka, Appl. Catal. 70 (1991) 175.
[7] N. Mizuno, M. Tateishi and M. Iwamoto, Appl. Catal. 128 (1995) L165.
[8] Y. Takita, H. Yamashita and K. Moritaka, Chem. Lett. (1989) 1733.
[9] W. Ueda and Y. Suzuki, Chem. Lett. (1995) 541.
[10] K. Otsuka, Y. Uragami and M. Hataro, Catal. Today 13 (1992) 667.
[11] M. Ai, J. Catal. 101 (1986) 389.
[12] S.T. Oyama, A.M. Middlebrook and G.A. Somorjai, J. Phys. Chem. 94 (1990) 5029.
[13] A. Erdöhelyi and F. Solymosi, J. Catal. 123 (1990) 31.
[14] Y.S. Yoon, N. Fujikawa, W. Ueda, Y. Moro-oka and K.W. Lee, Catal. Today 24 (1995) 327.
[15] R. Grabowski, B. Grzybowska, A. Kozlowska, J. Stoczynski, K. Wcislo and Y. Barbaux, Topics Catal. 3 (1996) 277.
[16] K. Marcinkowska, S. Kaliaguine and P.C. Roberge, J. Catal. 90 (1984) 49.
[17] K. Wada, K. Yoshida, Y. Watanabe and T. Suzuki, J. Chem. Soc. Chem. Commun. (1991) 726.
[18] N. Djeghri, M. Formenti, F. Juillet and S.J. Teichner, Faraday Discussions Chem. Soc. 58 (1974) 185.
[19] K. Iguchi, Y. Oshima and S. Koda, J. Photochem. Photobiol. A 80 (1994) 439.
[20] T. Hayakawa, K. Sato, T. Tsunoda, K. Suzuki, M. Shimizu and K. Takehira, J. Chem. Soc. Chem. Commun. (1994) 1743.
[21] A. Sen, M.A. Benvenuto, M. Lin, A.C. Hutson and N. Basickes, J. Am. Chem. Soc. 116 (1994) 998.
[22] I.P. Stolarov, M.N. Vargaftik, D.I. Shishkin and I.I. Moiseev, J. Chem. Soc. Chem. Commun. (1991) 938.
[23] J.E. Lyons and P.E. Ellis Jr., in: *Metalloporphyrins in Catalytic Oxidation*, ed. R.A. Sheldon (Dekker, New York, 1994) ch. 10.
[24] F. Blatter, H. Sun and H. Frei, Chem. Eur. J. 2 (1996) 385; Angew. Chem. Int. Ed. Engl. 35 (1996).
[25] H. Sun, F. Blatter and H. Frei, J. Am. Chem. Soc. 118 (1996) 6873.
[26] F. Blatter, H. Sun and H. Frei, Catal. Lett. 35 (1995) 1.
[27] D.W. Breck, *Zeolite Molecular Sieves: Structure, Chemistry and Use* (Wiley, New York, 1974).
[28] L. Bertsch and H.W. Habgood, J. Phys. Chem. 67 (1963) 1621.
[29] H.R. Williams and H.S. Mosher, Anal. Chem. 27 (1955) 517.
[30] R.S. Mulliken and W.B. Person, *Molecular Complexes* (Wiley, New York, 1969) ch. 14.
[31] E. Dempsey, in: *Molecular Sieves* (Society of Chemical Industry, London, 1968) p. 293.
[32] E. Preuss, G. Linden and M. Peuckert, J. Phys. Chem. 89 (1985) 2955.
[33] J.A.R. Coope, C.L. Gardner, C.A. McDowell and A.I. Pelman, Mol. Phys. 21 (1971) 1043.
[34] F. Blatter and H. Frei, to be submitted.
[35] B. Barrachin and E. Cohen de Lara, J. Chem. Soc. Faraday Trans. II 82 (1986) 1953.
[36] M. Iwasaki, K. Toriyama and K. Nunome, J. Am. Chem. Soc. 103 (1981) 3591.
[37] O. Hammerich and V.D. Parker, Adv. Phys. Org. Chem. 20 (1984) 55.
[38] J.A. Rabo, Catal. Rev. 23 (1981) 293.
[39] J.W. Ward, J. Phys. Chem. 72 (1968) 4211.
[40] J.W. Ward, in: *Zeolite Chemistry and Catalysis*, ACS Monograph 171, ed. J.A. Rabo (American Chemical Society, Washington, 1976) ch. 3.
[41] K.T. Geodokyan, A.V. Kiselev and V.I. Lygin, Russ. J. Phys. Chem. 41 (1967) 227, 476.
[42] A.A. Ukharskii, A.A. Kadushin, O.V. Al'tshuler and I.L. Tsitovskaya, Isv. Akad. Nauk. SSSR Ser. Khim. (1975) 765.
[43] D.L. Vanoppen, D.E. De Vos and P.A. Jacobs, Proc. 11th Int. Zeolite Conf., Seoul 1996.
[44] S. Korcek, J.H.B. Chenier, J.A. Howard and K.U. Ingold, Can. J. Chem. 50 (1972) 2285.